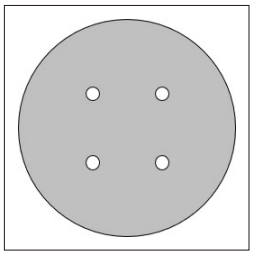

Measurement of Inter-core Crosstalk of Multicore Fibers with Optical Time Domain Reflectometry

Yuto KOBAYASHI*, Ayumi INOUE, Takahiro SUGANUMA,
Takuji NAGASHIMA, Tetsuya HAYASHI, and Takemi HASEGAWA

In multicore fiber (MCF) transmission, low inter-core crosstalk (XT) is crucial to suppress signal quality degradation. This study reveals that the dependence of the XT on fiber bending radius can be evaluated from the longitudinal changes in the bending radius of spooled MCFs with multi-channel OTDR. Using multi-channel OTDR, we also developed a measurement method for backscattered XT, which needs to be considered for bidirectional MCF transmission. With the developed method, we verified the validity of the theoretical prediction of the fiber length dependence of the backscattered XT and clarified the effect of fanout on the bidirectional XT. Our study shows the applicability of multi-channel OTDR for characterizing longitudinal XT change in MCFs and the preferable characteristics of bidirectional transmission in MCF.

Keywords: multicore fiber, crosstalk, OTDR, space division multiplexing

1. Introduction

In recent years, global telecommunications traffic has continued to grow at an annual rate of 30% as smartphones, live streaming, and online conferencing have become more common.[1] Meanwhile, the single-mode optical fibers that make up today's communication networks are already reaching their fundamental limit of transmission capacity at the experimental level.[2],[3] To break through this limit, space division multiplexing (SDM) technology is attracting attention.[4] Among them, a multicore fiber (MCF), which has multiple cores in one fiber is the most promising technology that is closest to practical application.

In MCFs, signal power leakage (crosstalk, or XT) occurs between multiple cores, and suppressing this is important to maintain signal quality. For this reason, various theoretical predictions and experiments have been conducted.[5]-[8]

We have shown that the fiber length dependence of various types of XT can be measured using OTDR.*1 [9]-[11] In this paper, we report the results of OTDR measurements of the fiber bending diameter dependence of XT in MCF[9] and the fiber length dependence of XT due to backscattering[10], which is an issue during bidirectional transmission.

2. XT in MCF and OTDR Measurements of XT

XT is caused by the coupling between modes propagating in one core and modes propagating in another core. The strength of this coupling is expressed by the power coupling coefficient h. The power coupling coefficient is mainly determined by the strength of the confinement of the electric field to the core, the distance between core centers, the difference in propagating constants between cores, and the fiber bending diameter. When the XT is small enough ($hL \ll 1$), XT can be expressed as

$$XT = hL, \quad \cdots\cdots (1)$$

where L is the fiber length. As this equation, XT is proportional to the fiber length L with a power coupling coefficient h.[5],[6] XT is the ratio of the power of core 1, the coupling source, P_1, to the power of core 2, the coupling destination, P_2 (Fig. 1), as follows.

$$XT \equiv \frac{P_2}{P_1}. \quad \cdots\cdots (2)$$

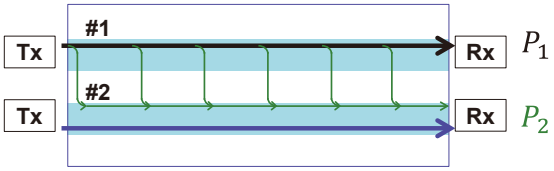

Fig. 1. Schematics of co-propagating XT[9]
TX: Transceiver, RX: Receiver

The XT can be measured from the ratio of the emitted light intensity of core 2 and core 1 at the end of the MCF when light is launched from the other end of the MCF to core 1 only (transmission power method). Alternatively, a measurement method using OTDR has also been proposed.[12] The measurement method using OTDR allows XT measurement at only one end of the MCF and the method using OTDR allows XT distribution measurement in the longitudinal direction of the fiber. Figure 2 shows schematics of XT measurement using OTDR. A test pulse launched from OTDR to core 1 of MCF is backscattered at the fiber longitudinal position z and it makes a round trip in MCF. Meanwhile, the pulse is coupled from core 1 to core 2 with a coefficient h both before and after backscattered. Since both core 1 and core 2 are similarly backscattered, there is no difference in power due to backscattered

between the cores. Therefore, the attenuation of light with backscattering can be excluded, and the XT measurement by OTDR simply measures the XT when the signal light travels twice the distance of the measurement position z, i.e. the XT can be expressed as

$$XT(z) \equiv \frac{1}{2}\frac{P_{12}(z)}{P_{11}(z)}, \quad \cdots\cdots (3)$$

where P_{11} (z) is the intensity of backscattered light of the launched core backscattered at position z, and P_{12} (z) is the intensity of backscattered light of the coupled core at possition z.

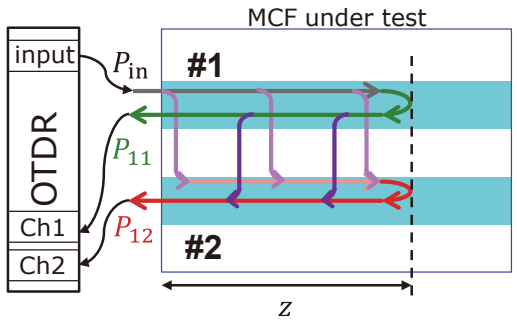

Fig. 2. Schematics of measuring XT in MCF using OTDR[9]

3. Measurement of the Bending Radius Dependence of XT in Heterogeneous Core Type MCF

XT varies with the bending radius of the fiber, which depends on the propagating constant difference between the cores of the MCF.[5] Measuring the bending radius dependence of XT is useful for estimating the XT at a given bending radius of cabling MCF. However, it is not efficient to measure the bending radius dependence of XT using the transmission method with MCF reels of various radii. We found that the bend radius dependence of XT can be efficiently measured using multi-channel OTDR (MC-OTDR) by using the bend radius changes from the inside to the outside of the reel.[9] In this section, we introduced the result of Ref. 9.

MC-OTDR was connected to MCF with FIFO*2 and the XT was measured with the measurement setup as shown in Fig. 3 (a). Measurements with the transmitted power method were also performed as reference measurements. Several heterogeneous uncoupled 2-core fibers with lengths from 13 to 60 km were used for the measurements. The outer diameter R_1 was measured from the outer circumference of the wound MCF and the bending radius R was calculated from the function of the fiber position from the end of the inside of the reel as follows

$$R = \{(1 - z/L)R_0^2 + (z/L)R_1^2\}^{1/2}, \quad \cdots\cdots (4)$$

where the bending radius R is assumed to be linear with respect to the number of turns, and the increment of the fiber length z is assumed to be linear with respect to R. The co-propagating XT was obtained using Eq. (1). The power coupling coefficient was obtained by differentiating the co-propagating XT by position.

Figure 4 shows the intensity of the backscattered pulse and co-propagating XT measured by MC-OTDR as a function of fiber longitudinal position z from inside to outside of the reel. The measurement was performed at a wavelength of 1550 nm and with a pulse width of 1.5 msec. In this measurement, the pulses were launched into MCF from the inside of reel (a) and from the outside of reel (b), respectively. From these results, the co-propagating XTs (c, d) from the launched end to position z were calculated as the method described above. These XTs agree well with the XTs measured by the transmission power method. Measurements by the transmission power method were made with the MCF connected to the FIFO and with the FIFO alone. These results correspond to the values at both ends of (c, d). The results from the transmission method agreed with the line measured by MC-OTDR with an average error of 0.2 dB. From (c, d), the relationship between position and co-propagating XT deviates from linear in the 0-10 km range.

Consequently, the fiber position dependence of the XT coefficient (power coupling coefficient) from this result is shown in Fig. 5 (a). The results measured from both ends of the MCF agree well. It supports the validity of the XT coefficient measurement using MC-OTDR. The variation of the XT coefficient along the fiber position can be

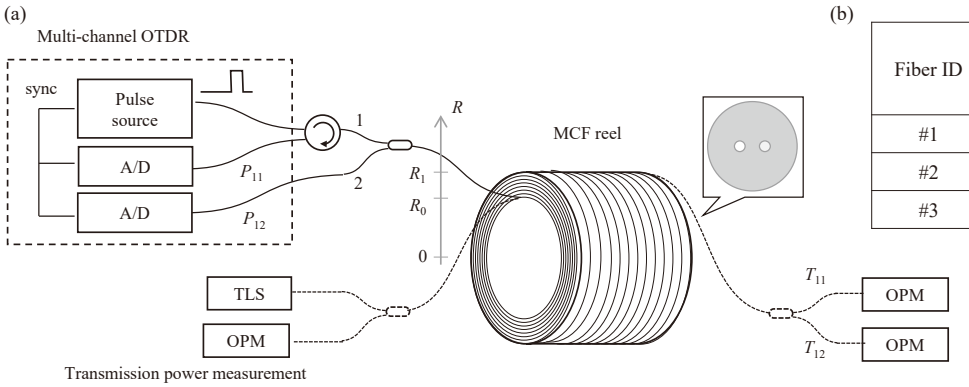

(b)

Fiber ID	Length [km]	XT [dB/100km]	
		Reel radius 87 mm	Reel radius 140 mm
#1	60.0	-25.3	-40.6
#2	52.9	N/A	-39.9
#3	13.4	-23.4	N/A

Fig. 3. (a) Schematics of the measurement of the bending radius dependence of XT in MCF using MC-OTDR[9]
TLS: tunable light source. OPM: Optical Power Meter. (b) The properties of the samples

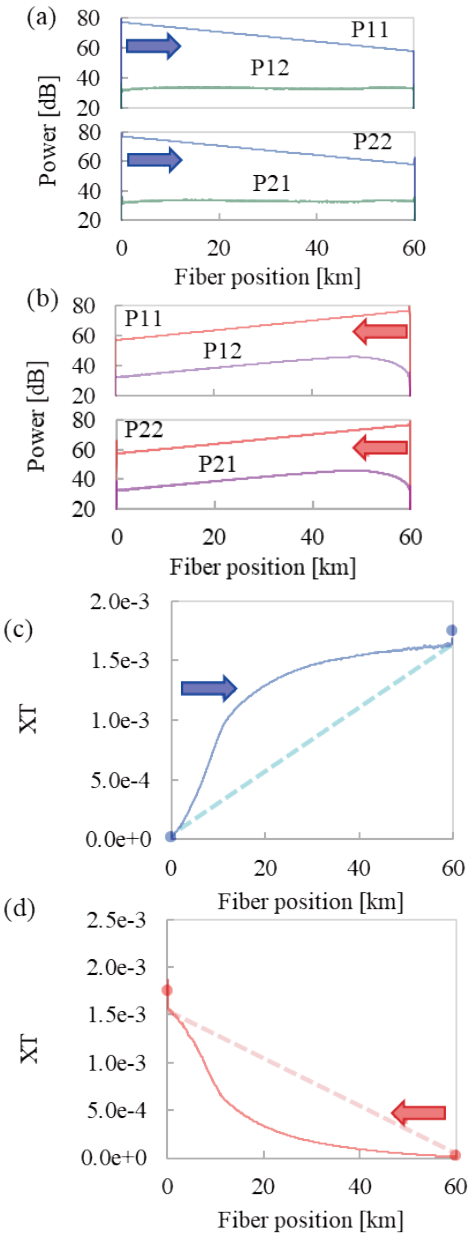

Fig. 4. The results of MC-OTDR[9]

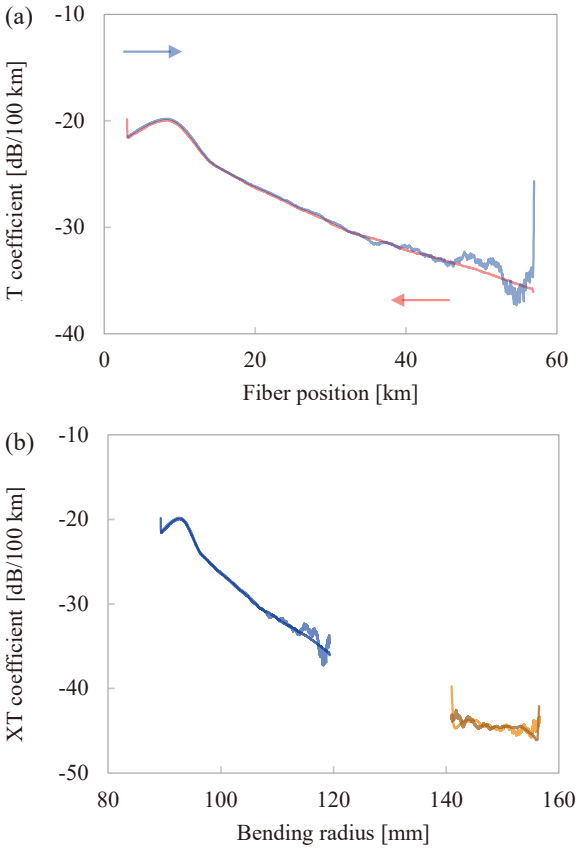

Fig. 5. (a) The fiber length dependence of the XT coefficient.[9] The arrows indicate the launching direction of the pulse. (b) The bending radius dependence of the XT coefficient.

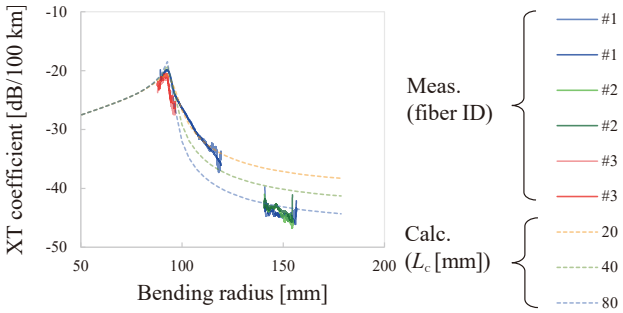

Fig. 6. The graph of the bending radius dependence of the XT coefficient measured by MC-OTDR

explained as a variation of the bending radius along the fiber position, as described later.

In order to investigate the dependence of XT on bending radius over a wide range of bending diameters, the MCFs under test were rewinding on a reel with a larger diameter. As shown in Fig. 5 (b), it can be confirmed that the XT between heterogenous cores decreases as the bending diameter increases.

Figure 6 shows the OTDR measurements of the XT coefficients and the theoretical calculation of the bending radius dependence of the XT coefficients using power coupling theory.[6],[13] The measured 2CF has a core-to-core propagation constant difference of 0.027%, a core pitch of 35 μm, and a correlation length L_c of between 20 and 80 mm. As seen in Fig. 6, the relationship between the XT coefficient and the bending radius is consistent with the calculation for any of the 20 to 80 mm. However, when the correlation length L_c is fixed to one, the measured and theoretical lines do not match for the entire length. This may be due to the change in correlation length with bending radius and the calculation accuracy of the propagation constant difference, which is an issue for future studies. In addition, we have used the $R_{eff} = 1.4R$ relationship in analogy with the photoelastic effect in bending loss. However, the value of 1.4 is a little high as a correction factor for the photoelastic effect, and this is also an issue for future studies.

4. Measurement of the Length Dependence of Backscattered XT

Until the previous section, we handled the XT which is considered to be the value when signal light propagates in the same direction between adjacent cores, as shown in Fig. 1 (here called co-propagating XT). However, XT can be reduced by counter-propagation of signal light between adjacent cores.[7],[8] XT during counter-propagation can be classified into three types by case: backscattered XT, reflected XT, and indirect XT.[7] In this section, we will discuss backscattered XT in particular.

Backscattered XT is a counter-propagating XT, which is caused by backscattering. Since backscattering can occur at any position in the longitudinal direction of the fiber, P_{bs2} in Fig. 7 can be expressed as the sum (integral) of the backscattered light at each position. The ratio of this P_{bs2} to the outgoing light P_1 of the coupled source core represents the backscattered XT,[7],[8]

$$XT_{bs} \equiv \frac{P_{bs2}}{P_1} = \frac{S\alpha_R}{\alpha} hL \left[\frac{\sinh(\alpha L)}{\alpha L} - \exp(-\alpha L) \right]. \quad \cdots\cdots (5)$$

The equation on the right-hand side is the theoretical expression for backscattered XT, where α is an attenuation constant of the fiber, S is the recapture factor of the Rayleigh scattering component to a backward direction, and α_R is the Rayleigh backscattering coefficient. As shown in Fig. 8, the dependence of backscattered XT on fiber length L changes at $1/\alpha$. XT_{bs} is proportional to L^2 in $L<<1/\alpha$ and is proportional to $\exp(\alpha L)$ in $L>>1/\alpha$. Compared to co-propagating XT, backscattered XT is more than 20 dB lower in the practical fiber length range. Therefore, propagating the signal light in the opposite directions is more advantageous for XT reduction than propagating in the same direction.

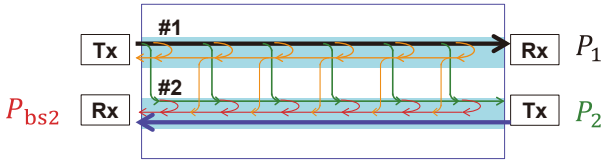

Fig. 7. Schematics of the backscattered XT[10]

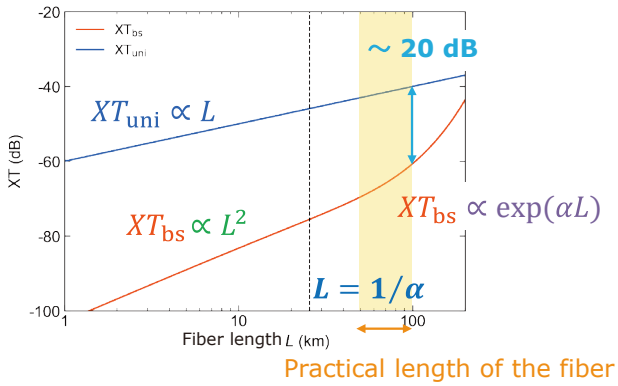

Fig. 8. The fiber length dependence of the backscattered XT[10]

We have proposed an OTDR-based measurement method for backscattered XT.[10] As already mentioned, the backscattered XT can be obtained by the ratio of the sum (integral) of the backscattered light at the coupled core to the transmitted light power of the coupling source core. Therefore, the integral of the backscattered light at each position of the coupled core can be replaced by the integration of OTDR-measured light $P_{12}(z)$. And the transmitted light at the coupling source can be replaced by $\sqrt{P_{11}(z)}$ which is converted to half the distance from the value of $P_{11}(z)$. Therefore, the backscattered XT can be expressed as

$$XT_{bs} \equiv \frac{S\alpha_R}{\sqrt{P_{11}(0)}} \frac{\int_0^z P_{12}(z')dz'}{\sqrt{P_{11}(z)}}. \quad \cdots\cdots (6)$$

The experimental system is shown in Fig. 9 (a). The pulse signal from the laser diode (LD) is launched into core 1 of the fiber under test via a FIFO, and the backscattered light from core 1 and core 2 is detected via the same FIFO. For comparison, the co-propagating XT and backscattered XT values were also measured in the experimental system shown in Fig. 9 (b) using a continuous wavelength (CW) tunable light source (TLS) with direct power measurements by the transmission method.[14]

Table 1 summarizes the characteristics of the measured samples. Both MCF-1 and MCF-2 were measured over a long span with fusion connection points. The FIFO of MCF-1 was an etched fiber bundle type FIFO with trench-assisted MCF pigtail[15] and the FIFO of MCF-2 was a fused taper type FIFO.[16]

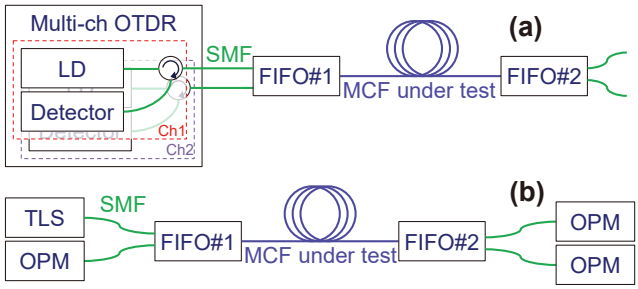

Fig. 9. (a) The XT measurement using with MC-OTDR.
(b) The measurement of XT with the power transmission method.
LD: Laser Diode, TLS Tunable Laser, OPM: Optical Power Meter.

Table 1. The properties of samples at λ= 1.55 μm[10]

	MCF-1	MCF-2
Number of cores	4	2
α in dB/km	0.19	0.16
A_{eff} [μm²]	74	109
R_{BS} in dB for 1-ns pulse W	-81	-84
Cutoff wavelength [μm]	< 1.53	< 1.53
Power coupling coeff. h in dB at 1 km [10 dB/decade]	-44.0[a]	-63.6[b]
Fiber length [km]	131	111
Fusion splice point [km]	44, 88	59
FIFO XT [dB]	< -80[a] (#1+#2)	-44.3 (#1)[b] -50.8 (#2)[b]

a: measured by power transmission method, b: measured by MC-OTDR.

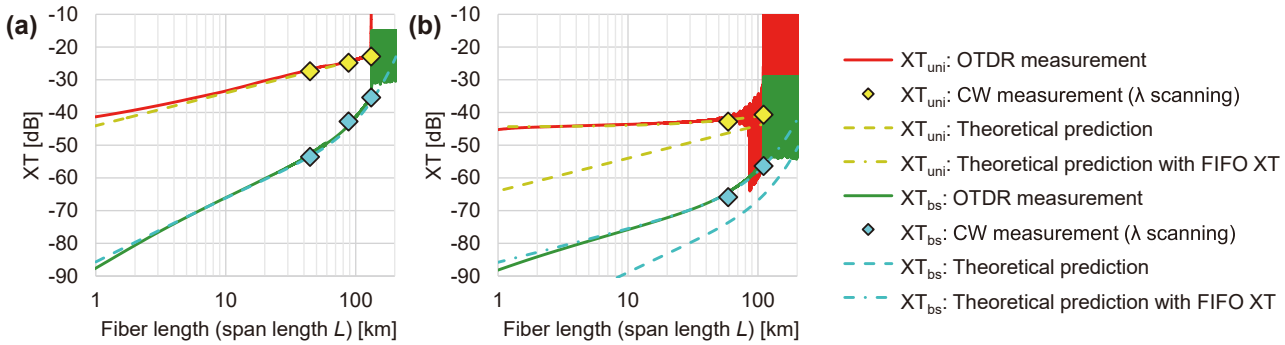

Fig. 10. fiber length dependence of XTs of (a)MCF-1 and (b) MCF-2[10]

Figure 10 (a) shows the accumulated XT values (in span) versus propagation distance at MCF-1. The pulse width of the OTDR pulse is 10 μs. The co-propagating XT and backscattered XT values were calculated using Eqs. (3) & (6). The zero point of the propagation distance was corrected by assuming that the pulse center enters the fiber at the zero point. The co-propagating XT and backscattered XT values from CW power measurements were also plotted. The theoretically predicted values of co-propagating XT were calculated using Eq. (1). The theoretical predictions of co-propagating XT were calculated using Eq. (1), where h was calculated from the results of the transmission method measurement at L = 131 km. The theoretical predictions for backscattered XT were also calculated using Eq. (5). The values in Table 1 were used in the calculations. (Thus, they are not the fitting curves of the measured backscattered XT.)

The OTDR measurements are in good agreement with the transmission method measurements. Furthermore, the longitudinal variation of co-propagating and backscattered XT measured by OTDR agrees very well with theoretical predictions. The discrepancy for L < 10 km is due to the fact that Eq. (6) does not fully account for the effect of the pulse width. However, for L > 10 km, the discrepancy is almost negligible, whose range covers the span length of most long-distance systems.

Figure 10 (b) shows the XT of MCF-2 versus propagation distance. The pulse width of the OTDR was set to 20 μs to increase sensitivity, since MCF-2 has a low XT even when propagated over long distances. Another measurement setup was as in the case of MCF-1. The XT of FIFO is not negligible and is almost the same as the XT of MCF-2 at 100 km.

Since the XT signal after 100 km was too weak to be measured even with 20 μs pulses, significant noise was observed in the OTDR XT measurements after propagation over 50 km. However, the trend of the OTDR measurements is in good agreement with that measured by the transmission method. No such noise was observed in the backscattered XT measured by OTDR because the backscattered XT is calculated from the integral of the XT component of the OTDR measurement and the weak power after long-distance propagation does not significantly affect the integral value.

The large difference between MCF-1 and MCF-2 measurements is the FIFO XT. The effect of FIFO cannot be ignored in MCF-2 measurements, and the co-propagating and backscattered XTs measured by OTDR do not agree with theoretical predictions.

Since co-propagating XT is linearly additive, the co-propagating XT including FIFO can be expressed as

$$XT_{\mathrm{uni}}^{\mathrm{MCF+FIFO}} = XT_{\mathrm{uni}}^{\mathrm{FIFO}} + hL. \quad \cdots\cdots (7)$$

Consequently, the backscattered XT affected by FIFO yields

$$XT_{BS}^{\mathrm{MCF+FIFO}} \approx XT_{\mathrm{BS}}^{\mathrm{MCF}} + 2XT_{\mathrm{uni}}^{\mathrm{FIFO}} \frac{S\alpha_R}{\alpha} \sinh(\alpha L). \quad \cdots\cdots (8)$$

The theoretical lines calculated based on this equation are in good agreement with the backscattered XT measured by OTDR.

5. Conclusion

Using XT measurement with MC-OTDR, the relationship between XT and bending radius can be evaluated. The XT measurement using OTDR is also useful for nondestructive measurement of length and bending radius dependence.

The newly devised method of measuring backscattered XT by OTDR verified that the backscattered XT in MCF agrees well with the prediction of the theoretical equation. Furthermore, it was shown that counter-propagating MCF transmission, in which the propagation direction is opposed between adjacent cores, is very effective in suppressing XT. The XT suppression of FIFO is also important for designing backscattered XT in counter-propagating MCF transmission systems, and the effect of XT in FIFO can be well estimated using the last equation in Section 4.

6. Acknowledgements

We would like to express our deepest gratitude to Professor Masataka Nakazawa and Associate Professor Masato Yoshida of the Research Institute of Electrical Communication, Tohoku University, for their cooperation and advice in the experiments.

This work was partially supported by the Ministry of

Internal Affairs and Communications (MIC)/Research and Development of Innovative Optical Network Technology for a Novel Social Infrastructure (JPMI00316) (Technological Theme II: OCEANS), Japan.

Technical Terms

∗1 OTDR: Optical Time Domain Reflectometry (OTDR) is a method that enables measurement of the longitudinal evolution of fiber attenuation of an optical fiber by launching a test pulse into the optical fiber and measuring its backscattered pulse in chronological order.

∗2 FIFO: Fan-In/Fan-Out (FIFO) is an optical device for optically connecting each core of an MCF to corresponding single-core fibers.

References

(1) "Cisco Visual Networking Index: Forecast and Trends, 2017–2022"
(2) R.-J. Essiambre and R. W. Tkach, "Capacity Trends and Limits of Optical Communication Networks," Proc. IEEE, vol. 100, no. 5, pp.1035-1055 (May 2012)
(3) A. Sano et al., "102.3-Tb/s (224 x 548-Gb/s) C- and extended L-band all-Raman transmission over 240 km using PDM-64QAM single carrier FDM with digital pilot tone," in Opt. Fiber Commun. Conf. (OFC), 2012, PDP5C.3
(4) P. J. Winzer and D. T. Neilson, "From Scaling Disparities to Integrated Parallelism: A Decathlon for a Decade," J. Lightw. Technol., vol. 35, no. 5, pp. 1099–1115 (Mar. 2017)
(5) T. Hayashi et al., "Design and fabrication of ultra-low crosstalk and low-loss multi-core fiber," Opt. Express, vol. 19, no. 17, pp. 16576–16592 (Aug. 2011)
(6) T. Hayashi et al., "Physical interpretation of intercore crosstalk in multicore fiber: effects of macrobend, structure fluctuation, and microbend," Opt. Express, vol. 21, No. 5, pp. 5401-5412 (Mar. 2013)
(7) T. Hayashi et al., "Uncoupled Multi-core Fiber Design for Practical Bidirectional Optical Communications," in Opt. Fiber Commun. Conf. (OFC), 2022, M1E.1
(8) T. Hayashi, "Accuracy of Analytical Expressions for Rayleigh Backscattered Crosstalk in Bidirectional Multi-Core Fiber Transmissions," Opt. Express, vol. 30, no. 13, pp. 23943–23952 (Jun. 2022)
(9) Y. Kobayashi et al., "Characterization of Inter-core Crosstalk of Multi-core Fiber as a Function of Bending Radius with Multi-channel OTDR," OptoElectron. Commun. Conf. / Photonics in Switching and Computing (OECC/PSC), 2022, TuC2-2
(10) Y. Kobayashi et al., "Distributed Measurement of Rayleigh Backscattered Crosstalk for Bidirectional Multicore Fiber Transmissions Using Multi-Channel Optical Time Domain Reflectometry," in Eur. Conf. Opt. Commun. (ECOC), 2022, Tu4A.3
(11) Y. Kobayashi et al., "Quadratically Suppressed Accumulation of Crosstalk Between Second Neighboring Cores of Multi-Core Fiber Measured by Commercial Single-Channel OTDR," Asia Commun. and Photonics Conf. / Int. Conf. on Info. Photonics and Opt. Commun. (ACP/IPOC), 2022, 2563
(12) M. Nakazawa et al., "Nondestructive measurement of mode couplings along a multi-core fiber using a synchronous multi-channel OTDR," Opt. Express, vol. 20, No. 11, pp.12530-12540 (May 2012).
(13) M. Koshiba et al., "Analytical expression of average power-coupling coefficients for estimating intercore crosstalk in multicore fibers," IEEE Photon. J., vol. 4, no. 5, pp. 1987–1995 (Oct. 2012)
(14) T. Hayashi et al., "Characterization of Crosstalk in Ultra-Low-Crosstalk Multi-Core Fiber," J. Lightw. Technol., vol. 30, no. 4, pp. 583–589 (Feb. 2012)
(15) T. Kikuchi et al., "Low insertion loss and high return loss fiber bundle fan-in/fan-out for four-core multi-core fiber," in OptoElectron. Commun. Conf./Photonics in Switching and Computing (OECC/PSC), 2022, TuC4-2
(16) V. I. Kopp et al., "Ultra-Low-Loss MCF Fanouts for Submarine SDM Applications," in Opt. Fiber Commun. Conf. (OFC), San Diego, 2022, Th1E.2

Contributors

The lead author is indicated by an asterisk (∗).

Y. KOBAYASHI*
• Optical Communications Laboratory

A. INOUE
• Optical Communications Laboratory

T. SUGANUMA
• Optical Communications Laboratory

T. NAGASHIMA
• Assistant Manager, Optical Communications Laboratory

T. HAYASHI
• Ph.D.
Group Manager, Optical Communications Laboratory

T. HASEGAWA
• Group Manager, Optical Communications Laboratory